CRYSTAL GROWTH & DESIGN

Article

pubs.acs.org/crystal

# 1,2,4,6-Thiatriazinyl Radicals and Dimers: Structural and Electronic Tuning through Heteroaromatic Substituent Modification

Nathan J. Yutronkie,[†,‡] Alicea A. Leitch,[†,‡] Ilia Korobkov,[†] and Jaclyn L. Brusso*[,†,‡]

[†]Department of Chemistry and [‡]Centre for Catalysis Research and Innovation, University of Ottawa, Ottawa, Ontario K1N 6N5, Canada

Supporting Information

**ABSTRACT:** The functionalization of thiatriazinyl (TTA) radicals with pyridyl and thienyl moieties is described, and their influence at both the molecular and solid-state level has been investigated. Comparative electron paramagnetic resonance studies of 3,5-bis-(2-pyridyl)-1,2,4,6-thiatriazinyl (**$Py_2$TTA**) and 3,5-bis-(2-thienyl)-1,2,4,6-thiatriazinyl (**$Th_2$TTA**) reveal the impact of heteroaromatic substitution on the electronic structure, which is supported by density functional theory calculations. Single crystal X-ray analysis emphasizes the importance of intermolecular contacts on the crystal packing and demonstrates the potential for structural control through S---N′ and N---HC′ interactions, which are enhanced in **$Py_2$TTA** and **$Th_2$TTA** by the presence of the pyridyl and thienyl groups, respectively. This work represents a fundamental study of heterocyclic aromatic substitution in thiazyl-based radicals and investigates how varying these functional groups influences the molecular properties and long-range order within the supramolecular structure.

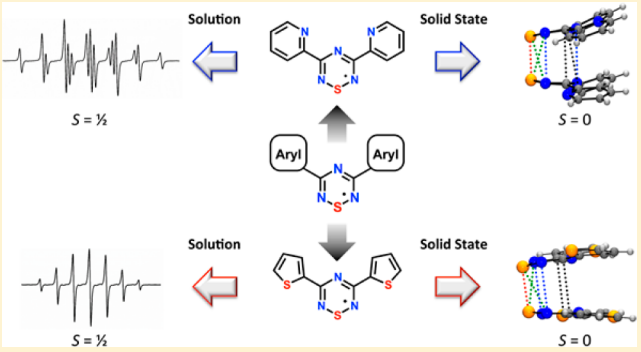


## INTRODUCTION

For some time stable radicals have been recognized as attractive building blocks in the development of molecular conductors and magnetic materials, in addition to their use as spin bearing ligands in transition metal complexes.[1−10] The exploration of organic and organo-main group radicals in the aforementioned applications represents a challenging yet fruitful research area, which drives the design and development of new open-shell materials. In that regard, heterocyclic thiazyl radicals are perhaps the most promising candidates as the S−N unit not only affords an unpaired electron, but the incorporation of heavy heteroatoms into planar $\pi$-conjugated frameworks also provides the potential for structural control through S---N′ and N---HC′ interactions and better opportunities for enhanced magnetic and electronic interactions by virtue of greater orbital overlap.[11−13] These features have attracted researchers in the direction of incorporating S−N moieties into $\pi$-conjugated frameworks, and a number of heterocyclic thiazyl radicals have been shown to crystallize as discrete radicals demonstrating interesting charge transport[14,15] and magnetic[15−18] properties. Others still have been reported to exhibit heat- and light-induced dimer-to-radical interconversions with potential applications in magnetic switches.[19,20]

Concerning their potential as spin bearing ligands, multidentate thiazyl radicals have proven to be an attractive building block.[21] In this regard, the thiatriazinyl radical (TTA) represents an archetypal system, as the general structure is ideal for the development of *N*-coordinate paramagnetic ligands. Furthermore, variation of the aromatic substituents, from phenyl groups to heterocycles containing nitrogen, oxygen, or sulfur, facilitates the development of chelating paramagnetic ligands, thus enabling coordination to a potentially diverse range of transition metals and lanthanides. The first report of a TTA radical was described by Markovskii et al. using electron paramagnetic resonance (EPR) spectroscopy;[22] however, it was not until 1984 that Oakley and coworkers first isolated and structurally characterized 3,5-bis-(phenyl)-1,2,4,6-thiatriazinyl (**$Ph_2$TTA**, Chart 1).[23] Since then, both symmetrically and asymmetrically substituted TTA

**Chart 1**

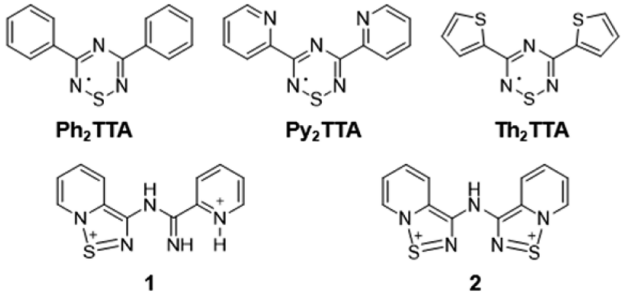


**Received:** March 2, 2015
**Revised:** March 30, 2015





DOI: 10.1021/acs.cgd.5b00296
*Cryst. Growth Des.* XXXX, XXX, XXX−XXX

radicals have been reported, most of which are partially functionalized by a phenyl group.[23−26] With respect to metal coordination, Boeré and co-workers have explored the reactivity of symmetric (**$Ph_2$TTA**) and asymmetric (3-phenyl-5-trifluoromethyl-TTA) derivatives with $[Cr(Cp)(CO_3)_2]$.[27,28] As may be expected, the substituents played a role in the coordination as **$Ph_2$TTA** afforded an $\eta^1$-adduct bonded through the sulfur atom, whereas the asymmetric ligand resulted in an $\eta^2$ S═N linkage. Interestingly, in both cases, coordination through the central nitrogen of the TTA ring did not occur. It is anticipated that heteroaromatic substituents, such as in **$Py_2$TTA** and **$Th_2$TTA** (Chart 1), would promote such coordination through the chelating effect rendering the N−S−N portion of the heterocyclic ring devoid of substituents. This would therefore permit these heteroatoms to engage in supramolecular interactions, which has been shown to direct crystal packing in the solid-state and facilitate conductive or magnetic exchange pathways in thiazyl based radical complexes.[21]

As a first step toward the development of heteroaromatic functionalized TTA, we recently reported the synthesis of **$Py_2$TTAH**, a task which involved the intermediacy of the mono- and bis-*N*-bridgehead-1,2,5-thiadiazolium salts **1** and **2**. This unusual noninnocent behavior of pyridyl nitrogens has only rarely been observed;[29] thus the apparent proclivity of the pyridyl ligands to form *N*-bridgehead-heterocycles represents an important finding and holds potential in the design of novel open and closed shell heterocyclic compounds. In our initial communication, the **$Py_2$TTA** radical was generated *in situ* and characterized by EPR spectroscopy. We have now successfully isolated and characterized **$Py_2$TTA** in the solid-state. In addition, the synthesis and characterization of the bis-thienyl derivative **$Th_2$TTA** are also reported herein. Comparison of the EPR spectra of the two radicals, along with computational studies, reveals the impact of heteroaromatic substitution on the electronic structure of TTA radicals. Moreover, crystal analysis emphasizes the importance of intermolecular contacts on the crystal packing and demonstrates the potential for structural control through S---N′ and N---HC′ interactions, which are significantly influenced by the presence of the pyridyl and thienyl groups in **$Py_2$TTA** and **$Th_2$TTA**, respectively. This work therefore represents a fundamental study of heterocyclic aromatic substitution in thiazyl-based radicals and investigates how varying these functional groups influences the molecular properties and long-range order within the supramolecular structure.

## RESULTS AND DISCUSSION

**Synthesis of $Py_2$TTA.** Our initial synthetic work en route to the closed-shell 3,5-bis-(2-pyridyl)-4-hydro-1,2,4,6-thiatriazine (**$Py_2$TTAH**) elucidated the preparation and structural characterization of two unusual *N*-bridgehead-1,2,5-thiadiazolium salts **1** and **2**.[30] While the *in situ* preparation of **$Py_2$TTA** through oxidation of **$Py_2$TTAH** with half an equivalent of iodine in the presence of 4-dimethylaminopyridine (DMAP) was successfully achieved, isolation of the radical in the solid state proved difficult due to the formation of intractable mixtures of DMAP salts. Initial attempts to overcome this problem included deprotonation of **$Py_2$TTAH** prior to oxidation in order to isolate the anionic derivative; however, the proton affinity of the central nitrogen on the TTA ring is quite high and, regardless of the base used (e.g., DMAP, proton sponge, KOH, etc.), generation of anionic **$Py_2TTA^-$** was unsuccessful. In fact, **$Py_2$TTAH** is surprisingly robust with a high tolerance toward aqueous, basic, and thermal conditions. Its only instability appears to be in acidic conditions, in which the thiatriazine ring opens and regenerates an *N*-bridgehead-1,2,5-thiadiazonium salt.[30]

Since deprotonation was not feasible, treatment with a relatively strong oxidant such as bromine was considered in order to prepare 3,5-bis-(2-pyridyl)-1-bromo-1,2,4,6-thiatriazine. This was not only expected to eliminate the problem associated with the proton on the central TTA ring, but also to provide a compound that can be treated with a suitable reductant to afford **$Py_2$TTA**, similar to the route employed for the phenyl-based derivatives.[23] However, while reaction with bromine formed the desired 1-bromo-1,2,4,6-thiatriazine, the generation of HBr led to protonation of the pyridyl nitrogen atoms affording the 3,5-bis-(2-pyridinium)-1-bromo-1,2,4,6-thiatriazine dication, isolated as a mixed bromide/tribromide salt (**3**, Scheme 1). Crystallization of this material from

**Scheme 1. Synthesis of the Bis-(2-pyridyl)-1,2,4,6-thiatriazinyl Radical**[a]

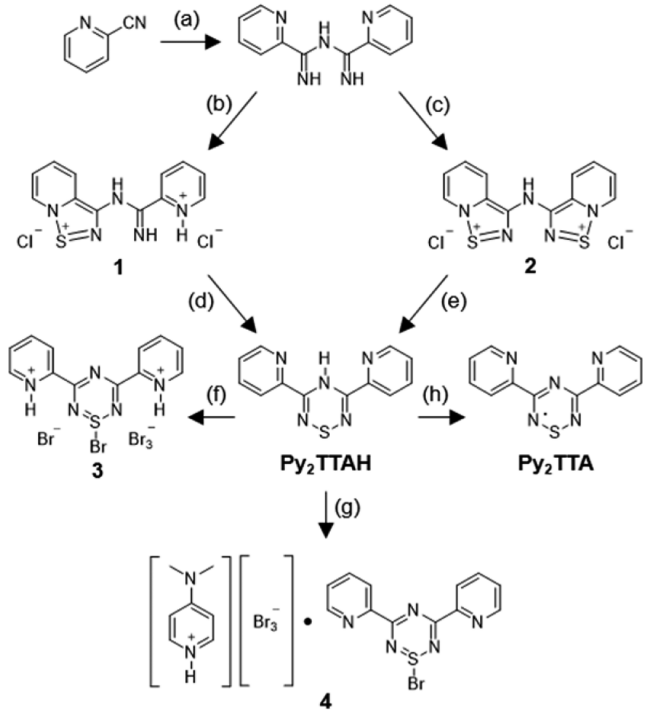


[a]Reagents and conditions: (a) $NH_3$, MeCN; (b) $S_2Cl_2$, MeCN, RT; (c) $S_2Cl_2$, MeCN, reflux; (d) PhCl, reflux; (e) $Ph_3Sb$, MeCN; (f) $Br_2$, MeCN, RT; (g) $Br_2$, MeCN, DMAP, reflux; (h) NCS, DMAP, MeCN, RT.

dichloroethane (DCE) afforded yellow needles suitable for X-ray analysis confirming the structural identity of **3** (Supporting Information, Figure S1).

To avoid protonation of the pyridyl nitrogen atoms, **$Py_2$TTAH** was treated with bromine in the presence of DMAP, affording the desired compound 3,5-bis-(2-pyridyl)-1-bromo-1,2,4,6-thiatriazine (**4**). However, while this confirmed that DMAP successfully inhibits protonation, the product **4** cocrystallized with DMAP·$HBr_3$ (Supporting Information, Figure S2), and attempts to reduce this mixed salt with triphenylantimony resulted in the regeneration of **$Py_2$TTAH**.

In order to isolate the **$Py_2$TTA** radical, we therefore turned to the use of oxidants, which would not generate protons as a


DOI: 10.1021/acs.cgd.5b00296
Cryst. Growth Des. XXXX, XXX, XXX−XXX

side-product. Oxygen, of course, also had to be avoided due to the proclivity of TTA radicals to form *N*-hydro-1-oxo-1,2,4,6-thiatriazines (Supporting Information, Figure S3). Various mild oxidants, including 2,3-dichloro-5,6-dicyanobenzoquinone (DDQ), *N*-bromosuccinimide (NBS), and *N*-chlorosuccinimide (NCS) were explored, and of these NCS proved to be the most effective affording **$Py_2TTA$** as a microcrystalline copper colored solid. Recrystallization of **$Py_2TTA$** from hot acetonitrile (MeCN) afforded crystals suitable for X-ray analysis (*vide infra*).

**Synthesis of $Th_2TTA$.** In regard to **$Th_2TTA$**, the absence of basic sites on the thienyl residue suggested that the synthesis would resemble that of the phenyl derivatives more closely than that of the pyridyl derivative. Nonetheless, regardless of the reaction pathway the most successful preparative routes include condensation of imidoylamidines with excess sulfur halides,[26,30,31] which therefore requires *N*-2-thienylimidoyl-2-thienylamidine (**5**) as a starting point. Although several preparative routes have been reported, unsubstituted *N*-imidoylamidines remain a synthetic challenge and have received relatively little attention in the literature. The classical route involves the reaction between an *N*-thioimidoylamidine with an amidine,[32] whereas an alternative avenue includes ring opening of triazines with lithium bis(trimethylsilyl)amide.[33] More recently, however, nitriles activated through inductive effects have been shown to undergo nucleophilic addition reactions with ammonia or amidine.[26,30,34] Our initial attempts to prepare **5** therefore focused on the reaction of 2-cyanothiophene with $NH_3$(g), which proved successful for the pyridyl derivative *N*-2-pyridylimidoyl-2-pyridylamidine.[30] Unfortunately, negligible yields of the desired product were obtained regardless of the temperature or pressure conditions used. This may be attributed to the electron donating character of the thiophene moiety, which deactivates the nitrile to nucleophilic addition. Similar challenges were encountered when effort was directed toward the reaction between the free-base 2-thienylamidine with 2-cyanothiophene. This was overcome by strengthening the nucleophilicity of the amidine through deprotonation via lithium diisopropylamide (LDA) affording **5** as a brown oil. Although this route can be used to prepare **5**, isolation of *N*-2-thienylimidoyl-2-thienylamidine was problematic leading to relatively poor purified yields. This was alleviated by changing the base to sodium hydride and employing a very polar aprotic solvent (e.g., DMSO),[35] affording **5** in much higher yields and greater purity. Subsequent condensation of **5** with excess sulfur monochloride afforded 3,5-bis-(2-thienyl)-1-chloro-1,2,4,6-thiatriazine (**6**) as a bright yellow crystalline material (Scheme 2). Because of its limited stability, **6** was used directly without further purification in the reduction reaction with triphenylantimony resulting in a dark green microcrystalline solid. Crystallization from hot DCE afforded **$Th_2TTA$** as dark red platelets suitable for single crystal X-ray analysis.

**EPR Spectroscopy.** We previously reported the *in situ* EPR spectrum of **$Py_2TTA$** in dichloromethane (DCM), which consisted of a complex multiplet that was simulated using a model based on hyperfine coupling to two equivalent and one unique $^{14}$N nuclei (experimentally derived constants: $a_N$ = 0.372 mT; $a_N$ = 0.427 mT; calculated coupling constants: $a_N$ = 0.347 mT; $a_N$ = 0.420 mT).[30] Interestingly, when recrystallized **$Py_2TTA$** was dissolved in degassed DCM, the solution remained EPR silent. While this finding was initially surprising, an EPR spectrum consistent with that obtained from *in situ* preparation of **$Py_2TTA$** was eventually achieved by switching to hot toluene (Figure 1), which was necessary to provide the elevated temperatures required to dissolve **$Py_2TTA$**. By contrast, the X-band EPR spectrum of **$Th_2TTA$** recorded in DCM at room temperature was much more easily obtained, indicating that dissolution and/or dissociation of **$Th_2TTA$** is clearly more extensive than in the case of **$Py_2TTA$**. The EPR for **$Th_2TTA$** exhibits a seven-line pattern that is consistent with the DFT calculated spin distribution for a TTA radical. It was simulated using a model based on hyperfine coupling to three quasi-equivalent $^{14}$N nuclei ($a_N$ = 0.392 mT and 0.386 mT), which may be compared with DFT calculated values ($a_N$ = 0.377 mT and 0.367 mT). The near equivalence of the $a_N$ values here is in contrast to **$Py_2TTA$** (see Figure 1) and is consistent with the expected electronic differences between the thienyl and pyridyl ligands, the latter being a more potent

**Scheme 2. Synthesis of the Bis-(2-thienyl)-1,2,4,6-thiatriazinyl Radical[a]**

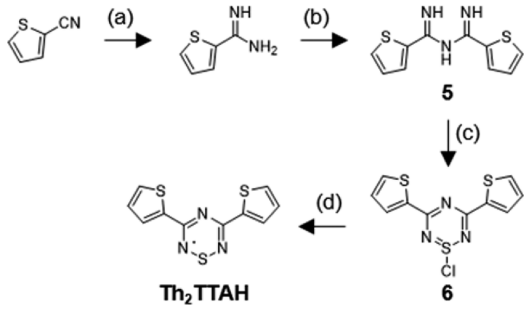


[a]Reagents and Conditions: (a) (i) NaOMe, MeOH, RT; (ii) $NH_4Cl$; (b) NaH, 2-thiophenecarbonitrile, DMSO, RT; (c) $S_2Cl_2$, MeCN, reflux; (d) $Ph_3Sb$, MeCN, RT.

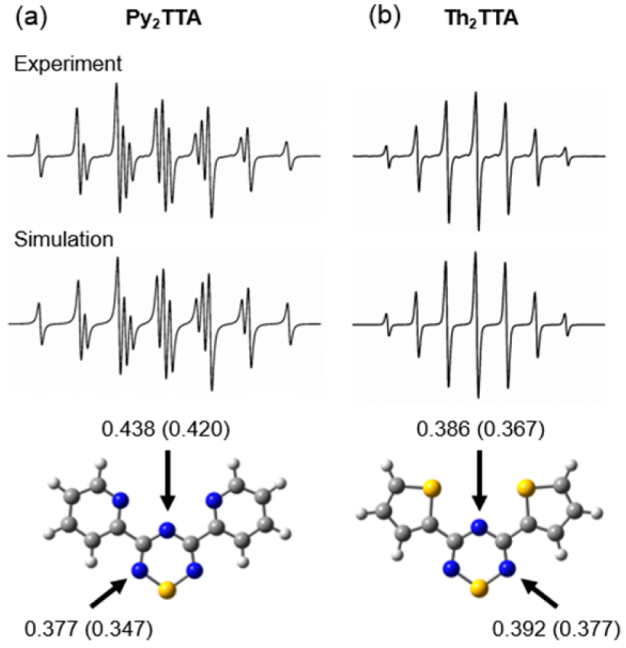


**Figure 1.** Experimental (top) and simulated (middle) EPR spectrum of (a) **$Py_2TTA$** in toluene collected at 40 °C ($g$ = 2.0068; SW = 3.5 mT; LW = 0.024 mT) and (b) **$Th_2TTA$** in DCM collected at RT ($g$ = 2.0066; SW = 3.5 mT; LW = 0.019 mT). (bottom) Experimentally derived and UB3LYP/EPR-II/6-31G(d)//UB3LYP/6-311G(d,p) calculated (in parentheses) coupling constants $a_N$ (in mT).



DOI: 10.1021/acs.cgd.5b00296
*Cryst. Growth Des.* XXXX, XXX, XXX−XXX

electron-withdrawing group. As a result, the **$Py_2TTA$** spin density is more extensively polarized away from the N−S−N region of the TTA core. Similar trends have been observed in the EPR spectra of *p*-substituted aryl TTA radicals.[25,36] For example, spin density in TTA systems is equally distributed over the three nitrogen atoms when phenyl or 4-$MeOC_6H_4$ substituents are employed, but becomes strongly polarized toward the central nitrogen atom (in the TTA ring) when electron-withdrawing 4-$NO_2C_6H_4$ groups are present (see Supporting Information Table S8).[25] Thus, comparison between the EPR spectra of **$Py_2TTA$** and **$Th_2TTA$** confirms the expectation that heterocyclic aromatic substitution influences the electronic structure of TTA radicals. Furthermore, this study also speaks to the solubility and, accordingly, the strength of intermolecular interactions observed in the pyridyl derivative compared to that of **$Th_2TTA$**, which is further exemplified by inspection of the crystal structures (*vide infra*).

**X-ray Crystallography.** To explore the impact of heteroaromatic substitution (i.e., pyridyl vs thienyl) on crystal packing, single crystals of **$Py_2TTA$** and **$Th_2TTA$** were analyzed by X-ray diffraction (Table 1). Two views of the solid-state

**Table 1. Crystal Data for $Py_2TTA$ and $Th_2TTA$**

| | $Py_2TTA$ | $Th_2TTA$ |
|---|---|---|
| formula | $C_{24}H_{16}N_{10}S_2$ | $C_{20}H_{12}N_6S_6$ |
| fw | 508.59 | 528.72 |
| crystal system | triclinic | monoclinic |
| space group | $P\bar{1}$ | $P2_1/n$ |
| $a$ (Å) | 8.3797(3) | 11.3840(6) |
| $b$ (Å) | 10.5524(3) | 10.7358(6) |
| $c$ (Å) | 13.0609(4) | 17.9318(9) |
| $\alpha$ (deg) | 81.4929(12) | 90 |
| $\beta$ (deg) | 84.0073(13) | 98.461(3) |
| $\gamma$ (deg) | 75.1622(12) | 90 |
| $V$ (Å$^3$) | 1101.45(6) | 2167.7(2) |
| $Z$ | 2 | 4 |
| $D_{calc}$ (mg/m$^3$) | 1.533 | 1.620 |
| $T$ (K) | 200 | 200 |
| $\mu$ (mm$^{-1}$) | 0.281 | 0.993 |
| $2\theta_{max}$ (deg) | 28.304 | 24.812 |
| no. of total reflections | 15900 | 25114 |
| no. of unique reflections | 5341 | 3671 |
| $R_{int}$ | 0.0229 | 0.0629 |
| $R_1$, $wR_2$ (on $F^2$) | 0.0412, 0.1024 | 0.0462, 0.0996 |

structures, that of the cofacial $\pi$-dimer and dimer-of-dimers (i.e., tetramers), are shown in Figure 2. Focusing on the molecular framework, a number of similarities exist between the two compounds. For example, crystals of **$Py_2TTA$** and **$Th_2TTA$** consist of discrete pairs of TTA rings linked in a cofacial manner containing short S---S contacts of 2.592(6) Å and 2.647(1), respectively. While these distances are longer than a disulfide bond (2.06 Å in $S_8$),[37] they are substantially shorter than the sum of the van der Waals radii (3.6 Å)[38] and are comparable to the transannular S---S interactions often observed in binary sulfur nitrides, which range from 2.43 to 2.65 Å (e.g., 2.43 Å for bis-$(Me_2N)_2$-DTTA;[39] 2.58 Å for $S_4N_4$).[40] As well, since the two TTA rings are perfectly eclipsed, numerous close S---N, N---N, and C---C interactions exist within the dimer as a result of the close S---S contact (see Supporting Information Table S1). In the structure of both **$Py_2TTA$** and **$Th_2TTA$**, the two TTA rings that form the cofacial dimer exhibit shallow boat-like configurations due to a slight displacement of the nitrogen and sulfur atoms that reside along the center of the molecular framework (i.e., the sulfur and nitrogen atom para to it). It is interesting to note that similar structural features (e.g., cofacial dimer, boat-like configuration) were described for the phenyl derivative **$Ph_2TTA$**,[23] indicative of minimal structural variation of the TTA ring and cofacial dimers upon heterocyclic substitution.

While a number of similarities exist between the structures of **$Py_2TTA$** and **$Th_2TTA$**, the impact of heteroaromatic substitution becomes apparent when looking at the supramolecular contacts, which direct packing in the solid state. For example, within the asymmetric unit of **$Py_2TTA$**, which belongs to the triclinic space group $P\bar{1}$ and contains two molecules, many unique close contacts that are within or nominally larger than the sum of the van der Waals separation exist,[38,41] whereas crystals of **$Th_2TTA$** belong to the monoclinic space group $P2_1/n$ and consists of fewer intermolecular interactions (see Supporting Information, Tables S3−S6). Although both compounds form tetramers in the solid state, in **$Py_2TTA$** these head-to-head dimer-of-dimers are held together by numerous S---N′ interactions, whereas only one S---S′ and three unique S---N′ contacts exist in the structure of **$Th_2TTA$** (Figure 2 and Supporting Information, Table S4). Furthermore, the tetramers of **$Py_2TTA$** form a brick-like array held together by a series of close $\pi$-contacts between the carbon atoms on the pyridyl rings and either the pyridyl or TTA ring on adjacent tetramers (Figure 3). A bird's-eye view of the **$Py_2TTA$** brick-like array reveals additional close contacts, many of which stem from hydrogen bonding between adjacent pyridyl rings, holding the molecules together in a 2D fashion (Figure 3c).

Similar to **$Py_2TTA$**, tetramers of **$Th_2TTA$** also form a brick-like arrangement held together primarily through $\pi-\pi$ interactions (e.g., C---C′ and C---S′); however, contrary to **$Py_2TTA$**, the structure of **$Th_2TTA$** consists of alternating layers of $\pi$-stacked tetramers that are rotated with respect to one another by 51.60(7)° forming a cross-braced configuration (Figure 4a). These layers are held together through lateral N---H′, S---H′, and S---C′ interactions (Figure 4b). While a number of contacts exist within the thienyl derivative, there are fewer than that of the pyridyl derivative. Such structural features may explain the enhanced solubility and presence of an EPR signal for **$Th_2TTA$** compared with **$Py_2TTA$**, which is EPR silent at room temperature. While the electron-withdrawing vs donating substituents have little structural impact on the molecular framework of the thiatriazinyl rings, heteroaromatic substitution (i.e., pyridyl vs thienyl) significantly influences the long-range molecular order and, therefore, the supramolecular architectures. This finding is further supported by comparing the crystal packing of the phenyl derivative (**$Ph_2TTA$**) with that of the pyridyl (**$Py_2TTA$**) and thienyl (**$Th_2TTA$**) analogues, where even fewer supramolecular contacts exist.[23]

## SUMMARY AND CONCLUSIONS

The isolation and solid-state characterization of **$Py_2TTA$** has now been achieved. In addition, the thienyl derivative **$Th_2TTA$** was prepared and structurally characterized. From a synthetic standpoint, the nature of the heteroatom in the aromatic substituents plays a pivotal role in the preparative pathway. On the basis of the results described here, the generation of a wide range of heteroaromatic TTA derivatives can be anticipated. Comparison of the EPR spectra along with computational


DOI: 10.1021/acs.cgd.5b00296
Cryst. Growth Des. XXXX, XXX, XXX−XXX

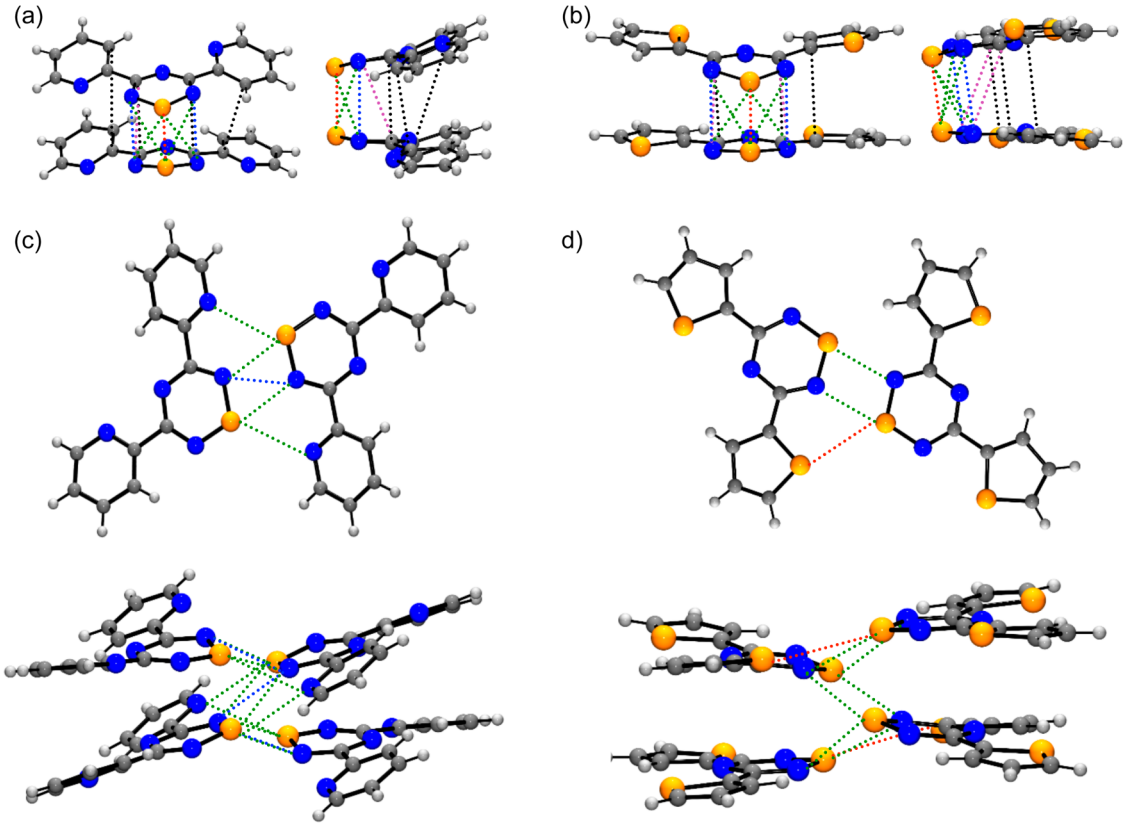


**Figure 2.** Two views of the dimer (a, b) and dimer-of-dimers (c, d) for **$Py_2TTA$** (a, c) and **$Th_2TTA$** (b, d) are shown with close intermolecular contacts highlighted by dashed lines. S---S′ contacts are shown in red; C---C′ in black; N---N′ in blue; S---N′ in green; C---N′ in purple.

studies demonstrates the effect of heteroaromatic substitution on the electronic structure, while crystal analysis emphasizes the importance of intermolecular contacts on the crystal packing. In this regard, although structural studies reveal several similarities between **$Py_2TTA$** and **$Th_2TTA$**, the presence of heteroatoms in the aromatic substituents significantly influences the crystal packing and, hence, the supramolecular architectures. The enhanced intermolecular interactions observed in **$Py_2TTA$** and **$Th_2TTA$** (compared to **$Ph_2TTA$**) result in more tightly bound structures, the consequence of which was particularly noted in the EPR studies of **$Py_2TTA$**, in which a purified sample requires hot toluene to produce an EPR signal.

Inclusion of heteroatoms in the aromatic substituents of TTA not only influences the molecular and solid-state properties of the discrete molecules, but it also facilitates coordination to a variety of metals. Not only is this anticipated to stabilize the unpaired electron thus preventing dimerization, but it also provides an avenue to generate coordination complexes that can take advantage of the unencumbered N−S−N portion of the TTA ring, which can engage in supramolecular interactions that are known to direct crystal packing in thiazyl based ligands and provide conductive and magnetic exchange pathways; such studies are currently being pursued. In regard to coordination chemistry, a logical next step would involve the preparation of the pyrimidyl derivative **$Pm_2TTA$** (Chart 2). Isolation of **$Pm_2TTA$** would not only facilitate multimetallic coordination, but the design of such a ligand has significant potential toward the development of extended coordination polymers and networks that contain spin-bearing ligands. In regard to the thienyl derivative, the availability of reactive $\alpha$-sites enable extension of the thienyl moieties such that oligothiophene functionalized TTA radicals may be realized. Accordingly, the current **$Th_2TTA$** system can act as a prototype for the construction of a large series of **$(Th_n)_2TTA$** derivatives. Preparation of the aforementioned pyrimidine and oligothiophene functionalized TTA radicals is currently underway.

## EXPERIMENTAL METHODS

**General Procedures and Starting Materials.** The reagents sulfur monochloride (Sigma-Aldrich) and triphenylantimony (TCI America) were obtained commercially and used as received. Sodium hydride (60% dispersion in mineral oil, Alfa Aesar) was washed with hexanes prior to use. Acetonitrile (MeCN) and 1,2-dichloroethane (DCE) were dried by distillation over $P_2O_5$ and stored over 4 Å molecular sieves. Dimethyl sulfoxide (DMSO) was dried and stored over 4 Å molecular sieves. 3,5-bis-(2-pyridyl)-4-hydro-1,2,4,6-thiatriazine (**$Py_2TTAH$**),[30] 2-thiophenecarbonitrile[42] and 2-thiophenecarboxamidine[43] were prepared as outlined in the literature. All reactions were performed under an atmosphere of dry nitrogen. Melting points are uncorrected. $^1$H NMR and $^{13}$C NMR spectra were run in $CDCl_3$ solutions at room temperature on the Bruker Avance 400 MHz and Bruker Avance 300 MHz spectrometers. IR spectra of solid samples were recorded on an Agilent Technologies Cary 630 FT-IR spectrometer. Elemental analyses were performed by MHW Laboratories, Phoenix, AZ 85018.

**EPR Spectroscopy.** The X-band EPR spectra of **$Th_2TTA$** was recorded at ambient temperature using a Bruker EMX-200 spectrometer on samples dissolved in degassed dichloromethane and/or toluene. Hyperfine coupling constants were obtained by spectral simulation using PEST Winsim and Bruker WinEPR Simfonia.[44]

**Crystal Growth.** Yellow needles of **3** suitable for X-ray analysis were grown by slowly cooling a saturated DCE solution. Orange


DOI: 10.1021/acs.cgd.5b00296
Cryst. Growth Des. XXXX, XXX, XXX−XXX

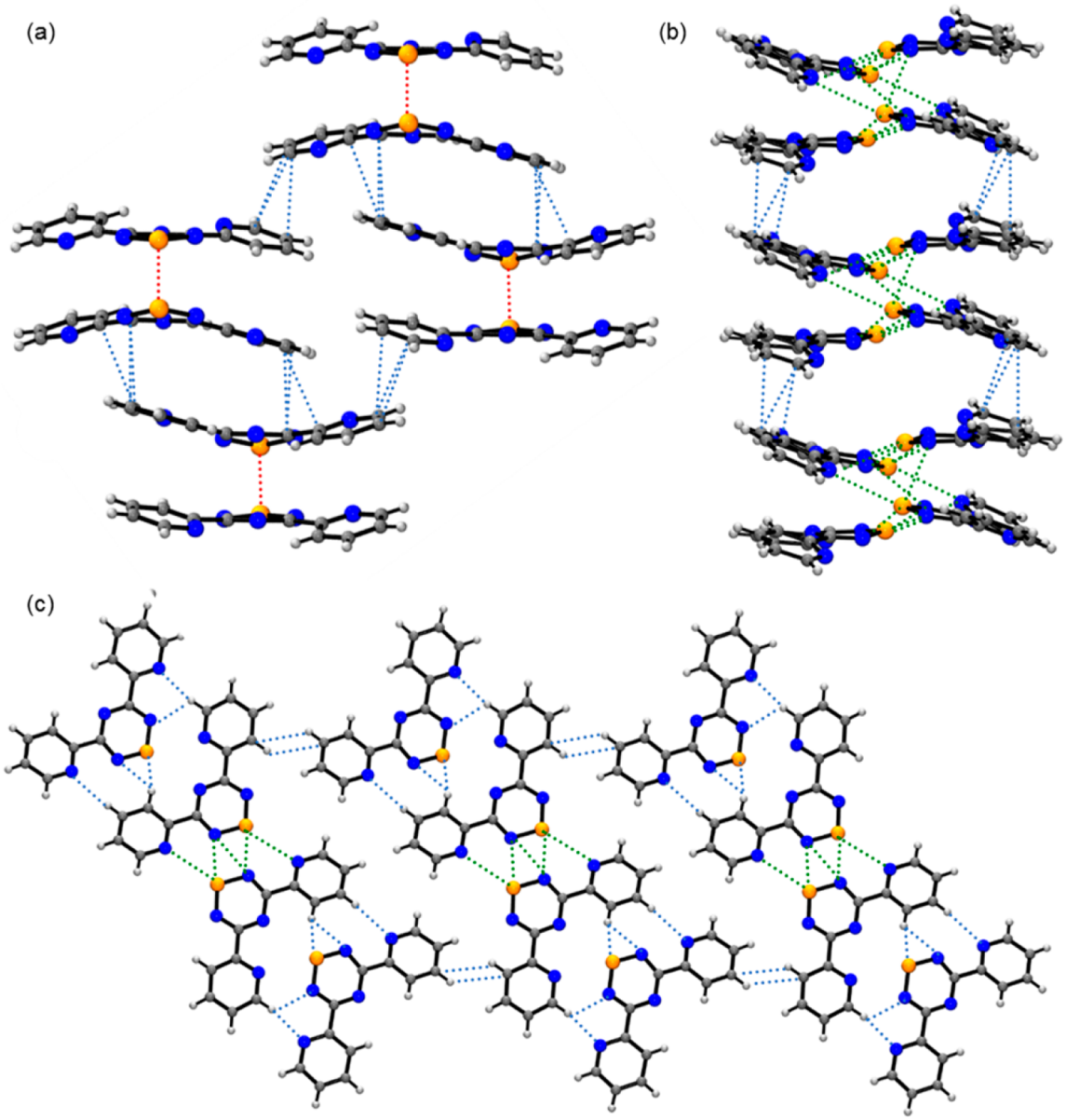


**Figure 3.** Two views of the packing arrangement exhibited by crystals of **$Py_2TTA$** demonstrating the (a) brick-like array and (b) superimposed $\pi$-stacked tetramers with $\pi-\pi$ interactions between adjacent tetramers highlighted by blue dashed lines. (c) Bird's-eye view of the packing arrangement of **$Py_2TTA$** illustrating the N---H′ contacts (blue dashed lines) holding the molecules together in a 2D network. S---S dimer contacts are shown in red; tetramer contacts in green.

blocks of **4** suitable for X-ray analysis were grown by slowly cooling a saturated MeCN solution. Black cubes of 3,5-bis-(pyridyl)-4-hydro-1-oxo-1,2,4,6-thiatriazine and transparent needles 3,5-bis-(thienyl)-2-hydro-1-oxo-1,2,4,6-thiatriazine suitable for X-ray analysis were grown by slowly cooling saturated MeCN solutions. Black blocks of **$Py_2TTA$** suitable for X-ray analysis were grown by slowly cooling a saturated MeCN solution. Red platelets of **$Th_2TTA$** suitable for X-ray analysis were grown by slowly cooling a saturated DCE solution.

**Crystallography.** The data collection results for compounds **3**, **4**, 3,5-bis-(pyridyl)-4-hydro-1-oxo-1,2,4,6-thiatriazine, 3,5-bis-(thienyl)-2-hydro-1-oxo-1,2,4,6-thiatriazine, **$Py_2TTA$** and **$Th_2TTA$** represent the best data sets obtained in several trials for each sample. The crystals were mounted on thin glass fibers using paraffin oil. Prior to data collection, crystals were cooled to 200.15 K. The data were collected on a Bruker AXS KAPPA single crystal diffractometer equipped with a sealed Mo tube source (wavelength 0.71073 Å) and APEX II CCD detector. The raw data collection and processing were performed with the APEX II software package from BRUKER AXS.[45] The diffraction data for crystals of **3**, 3,5-bis-(thienyl)-2-hydro-1-oxo-1,2,4,6-thiatriazine and **$Th_2TTA$** were collected with a sequence of 0.3° $\omega$ scans at 0, 120, and 240° in $\varphi$. Because of the lower unit cell symmetry, in order to ensure adequate data redundancy, diffraction data for **4**, 3,5-bis-(thienyl)-2-hydro-1-oxo-1,2,4,6-thiatriazine and **$Py_2TTA$** were collected with a sequence of 0.3° $\omega$ scans at 0, 90, 180, and 270° in $\varphi$. The initial unit cell parameters were determined from 60 data frames with 0.3° $\omega$ scan each, collected at the different sections of the Ewald sphere. Semiempirical absorption corrections based on equivalent reflections were applied.[46] Systematic absences in the diffraction data and unit cell parameters were consistent with triclinic $P\bar{1}$ (No. 2) for compound **4**, 3,5-bis-(pyridyl)-4-hydro-1-oxo-1,2,4,6-thiatriazine and **$Py_2TTA$**, monoclinic $P2_1/c$ (No. 14) for compound **3**, monoclinic $P2_1$ (No. 4) for 3,5-bis-(thienyl)-2-hydro-1-oxo-1,2,4,6-thiatriazine, and monoclinic $P2_1/n$ (No. 14, alternative settings) for **$Th_2TTA$**. Solutions in the centrosymmetric space groups for all the compounds except 3,5-bis-(thienyl)-2-hydro-1-oxo-1,2,4,6-thiatriazine yielded chemically reasonable and computationally stable results of refinement. Meanwhile,


DOI: 10.1021/acs.cgd.5b00296
*Cryst. Growth Des.* XXXX, XXX, XXX−XXX

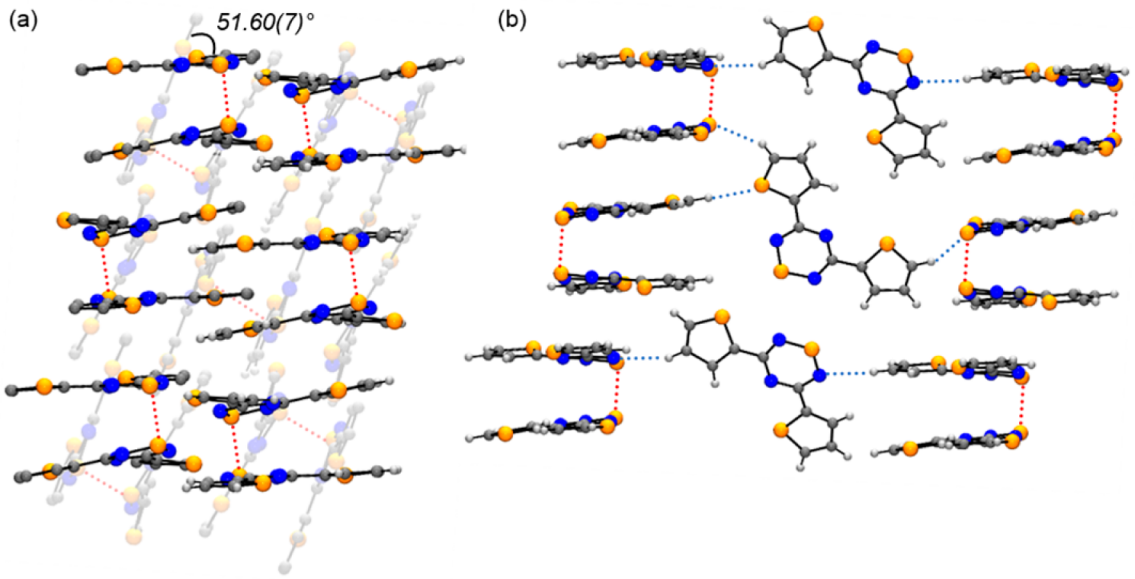


**Figure 4.** (a) The cross-braced arrangement found for **$Th_2$TTA**, which consists of alternating layers of $\pi$-stacked tetramers that are rotated with respect to one another by 51.60(7)°. (b) A 90° rotated view of (a) illustrating the lateral N---H′, S---H′, and S---C′ interactions (blue dashed lines) between the cross-braced layers. S−S dimer contacts are shown in red.

**Chart 2**

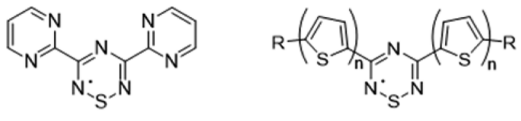

**$Pm_2$TTA** **$(Th_n)_2$TTA**

diffraction data for 3,5-bis-(thienyl)-2-hydro-1-oxo-1,2,4,6-thiatriazine suggested non-centrosymmetric space groups for the structural model. The structures were solved by direct methods, completed with difference Fourier synthesis, and refined with full-matrix least-squares procedures based on $F^2$.

The structural model for 3,5-bis-(pyridyl)-4-hydro-1-oxo-1,2,4,6-thiatriazine contains one target compound molecule located in general positions. An initial unit cell determination procedure suggested that the crystal mounted on the machine was non-merohedrally twinned. Refinement of the structure confirmed the presence of the second independent crystallographic domain. In order to find independent orientation matrices 5423 reflections were collected from 3 sets of 50 frames each in the different sections of the Ewald sphere. The collected reflection data were processed with CELL_NOW software[47] and produced two independent orientation matrices. The data set was reintegrated with two obtained matrices, treated for twinning absorption corrections, and consecutive model refinement was performed against HKLF 5 reflection data file. Twinning domain ratio coefficient (BASF) was refined to 0.4102.

The asymmetric unit for compound **4** includes two target molecules and one molecule of *para*-amino pyridine, all located in general positions. The structure also incorporates two $Br_3^-$ anions located in the two independent inversion centers.

The diffraction data for the crystal of the complex **3** were collected to 0.75 Å resolution. The absorption correction stage, that both R(int) and R(sigma) exceed 35% for the data below 0.85 Å resolution. On the basis of the R(sigma) value, data were truncated to 0.80 Å resolution for refinement. The asymmetric unit for this crystallographic model of **3** consists of one target compound molecule, one $Br_3^-$ anion, and one separate $Br^-$ atom. All the fragments are located in the general positions.

The structural model of **$Py_2$TTA** consists of two aligned molecules of the target compound with close contact between two sulfur atoms of the units (S(1)−S(2) = 2.59 Å). Both molecules are located in the general positions in the unit cell.

The asymmetric unit for the structure of 3,5-bis-(thienyl)-2-hydro-1-oxo-1,2,4,6-thiatriazine contains one target molecule located in a general position. On the final stages of refinement, the numbers suggested the presence of merohedral twinning in the structure. To take this into account, simple TWIN and BASF instructions were introduced, and the twinning parameter was refined to 0.0687. After introduction of anisotropic refinement parameters for all the non-hydrogen atoms, it was discovered that one of the five-member rings (S(3), C(7)−C(9)) of the structure is disordered by 180°-rotation around the C(2)−C(7) carbon−carbon bond. The atomic positions of this fragment were split to model the disorder, and occupancy was allowed to refine. On the latest stages of refinement, occupancy was fixed at 61% − 39% providing satisfactory anisotropic thermal motion parameters. To ensure proper geometry of the disordered moiety, a set of geometric restraints (SAME) were introduced.

The structural model for **$Th_2$TTA** demonstrates two molecules of the target compound located in the general position of the unit cell. Similar to the structure of **$Py_2$TTA**, these two molecules reveal close contact between two sulfur atoms (S(1)−S(4) = 2.65 Å). The anisotropic refinement of the structure revealed possible disorder by 180° rotation around the carbon bonds for all four of the five-member rings. To model the disorder, the positions of sulfur atoms within these five-member rings and the positions of carbon atoms opposite to sulfur were split, and the occupancy coefficients were allowed to refine. On the later stages of refinement, occupancy coefficients were fixed at the following values: S(2), C(3)−C(6) ring is rotated around C(1)−C(3) bond with partial occupancies 90%: 10%; S(3), C(7)−C(10) ring is rotated around C(2)−C(7) bond with partial occupancies 75%: 25%; S(5), C(13)−C(16) ring is rotated around C(11)−C(13) bond with partial occupancies 80%: 20%; S(6), C(17)−C(20) ring is rotated around C(12)−C(17) bond with partial occupancies 65%: 35%. To ensure proper fragments, geometries and acceptable anisotropic thermal displacement coefficients for two sets of geometry (SADI) and thermal motions (EADP) restraints were used during the refinement.

For all six compounds, positions of all hydrogen atoms were calculated based on the geometry of related non-hydrogen atoms. All hydrogen atoms were treated as idealized contributions during the refinement. All scattering factors are contained in several versions of


DOI: 10.1021/acs.cgd.5b00296
*Cryst. Growth Des.* XXXX, XXX, XXX−XXX

the SHELXTL program library, with the latest version used being v.6.12.[48]

*Preparation of 3,5-Bis-(2-pyridyl)-1,2,4,6-thiatriazinyl (**Py$_2$TTA**).* Under an inert atmosphere, **Py$_2$TTAH** (0.500 g, 1.96 mmol), 4-dimethylaminopyridine (0.136 g, 1.11 mmol) and *N*-chlorosuccinimide (0.134 g, 1.00 mmol) were combined and 5 mL of degassed MeCN (3 freeze−pump−thaw cycles) was added affording a maroon slurry. After 2 h, a fine brown solid was filtered *in vacuo* and washed twice with 3 mL of MeCN. Crude yield = 0.175 g (0.688 mmol, 35%). Recrystallization from MeCN afforded black-brown microcrystalline material. IR: $\upsilon_{max}$ ($cm^{-1}$): 3050 (w), 3004 (w), 1641 (w), 1571 (w), 1530 (m), 1510 (m), 1489 (m), 1476 (m), 1461 (m), 1422 (m), 1396 (m), 1380 (s), 1345 (m), 1254 (m), 1231 (m), 1160 (w), 1112 (m), 1042 (w), 994 (m), 974 (w), 912 (w), 843 (w), 814 (w), 768 (s), 757 (m), 739 (s), 726 (s), 692 (m), 668 (w). Anal. Calcd for $C_{12}H_8N_5S$: C, 56.68; H, 3.17; N, 27.54. Found: C, 56.90; H, 3.37; N, 27.66.

*Preparation of N-2-Thienylimidoyl-2-thienylamidine (**3**).* Sodium hydride (1.71 g, 71.3 mmol) was added to a DMSO (86 mL) solution of 2-thiophenecarboxamidine (6.00 g, 47.6 mmol) and 2-thiophenecarbonitrile (5.20 g, 47.6 mmol), initially releasing hydrogen gas. After stirring for 56 h at room temperature, the resulting dark brown solution was quenched with 200 mL of water and extracted with DCM. The organic phase was washed with water, dried over potassium carbonate, and then filtered, and the solvent was removed under reduced pressure affording **3** as a brown solid (9.26 g, 39.4 mmol, 83%). Pale yellow needles of **3** were obtained by recrystallization in hexanes. mp 98−99 °C, $^1$H NMR ($\delta$, $CDCl_3$): 7.51 (2H, dd, $J$ = 1.63, Ar), 7.46 (2H, dd, $J$ = 2.06, Ar), 7.09 (2H, dd, $J$ = 2.94, Ar), $^{13}$C NMR ($\delta$, $CDCl_3$): 162.09, 142.75, 130.10, 127.73, 126.43, IR $\nu_{max}$ ($cm^{-1}$): 3434.7 (m), 3263.3 (m), 1588.3 (s), 1522.5 (s), 1481.0 (s), 1422.6 (s), 1381.5 (s), 1319.7 (m), 1241.3 (w), 1167.1 (s), 1115.6 (w), 1046.8 (m), 978.2 (m), 910.2 (w), 856.2 (m), 826.8 (m), Anal. Calcd for $C_{10}H_9N_3S_2$: C, 51.04; H, 3.86; N, 17.86, Found: C, 51.16; H, 3.73; N, 17.74.

*Preparation of 1-Chloro-3,5-di(thien-2-yl)-1λ4,2,4,6-thiatriazine (**4**).* Sulfur monochloride (5.72 g, 42.4) was added dropwise to a stirring solution of **3** (2.0 g, 8.50 mmol) in 50 mL of dry acetonitrile forming a white precipitate, which dissolved upon heating to reflux. The resulting in a bright orange solution was hot filtered and, on cooling to 0 °C, yellow needle-like crystals formed. The crystals were filtered and dried under reduced pressure. Yield 2.07 g (7.22 mmol, 85%) $^1$H NMR ($\delta$, $CDCl_3$): 8.22 (2H, dd, $J$ = 1.70, Ar), 7.78 (2H, dd, $J$ = 2.06, Ar), 7.24 (2H, dd, $J$ = 2.94, Ar), $^{13}$C NMR ($\delta$, $CDCl_3$): 165.48, 140.85, 135.91, 134.38, 129.09, IR $\nu_{max}$ ($cm^{-1}$): 3101.5 (w), 1516.3 (s), 1477.6 (w), 1437.9 (m), 1395.8 (br, s), 1218.6 (s), 1112.7 (m), 1027.3 (br, s), 943.9 (br, m), 858.2 (s), 837.9 (m), 823.1 (m), 768.4 (s), 745.2 (m), 715.2 (s), 699.1 (s).

*Preparation of 3,5-Bis-(2-thienyl)-1,2,4,6-thiatriazinyl (**Th$_2$TTA**).* Triphenylantimony (1.22 g, 3.45 mmol) and **4** (2.07 g, 6.90 mmol) were dissolved in dry, degassed MeCN (three freeze−pump−thaw cycles) resulting in a maroon slurry. After stirring for 1 h, a dark purple solid was filtered *in vacuo*. Crude yield 1.66 g (3.14 mmol, 91%). Recrystallization from DCE afforded **Th$_2$TTA** as a dark red microcrystalline solid. dec >135 °C, IR $\nu_{max}$ ($cm^{-1}$): 3089.3 (w), 1519.2 (m), 1464.0 (m), 1418.1 (s), 1403.8 (s), 1369.9 (br, s), 1340 (s), 1328.1 (s), 1235.8 (m), 1195.7 (br, s), 1142.1 (w), 1126.3 (w), 1079.9 (m), 1052.0 (m), 1031.1 (s), 1015.4 (s), 1000.9 (s), 939.5 (m), 910.1 (w), 862.8 (m), 852.7 (m), 798.3 (br, m), 764.3 (s), 747.2 (s), 736.7 (s), 710.4 (br, s). Anal. Calcd for $C_{10}H_6N_3S_3$: C, 45.43; H, 2.29; N, 15,90, Found: C, 45.60; H, 2.47; N, 15.97.

## ■ ASSOCIATED CONTENT

### Supporting Information

Crystallography, EPR spectroscopy, and computational studies. This material is available free of charge via the Internet at http://pubs.acs.org.

## ■ AUTHOR INFORMATION


### Corresponding Author

*E-mail: jbrusso@uottawa.ca.


### Notes

The authors declare no competing financial interest.

## ■ ACKNOWLEDGMENTS

The authors wish to thank the University of Ottawa, the Canadian Foundation for Innovation, and the National Sciences and Engineering Council of Canada for financial support. N.J.Y. acknowledges support through an Ontario Graduate Scholarship.

## ■ REFERENCES


(1) Hicks, R. G. In *Stable Radicals: Fundamentals and Applied Aspects of Odd-Electron Compounds*; Hicks, R. G., Ed.; John Wiley & Sons, Ltd.: Wiltshire, U.K., 2010; pp 248−280.

(2) Ratera, I.; Veciana, J. *Chem. Soc. Rev.* **2012**, *41*, 303−349.

(3) Hicks, R. G. *Nat. Chem.* **2011**, *3*, 189−191.

(4) Cordes, A. W.; Haddon, R. C.; Oakley, R. T. *Phosphorus, Sulfur Silicon Relat. Elem.* **2004**, *179*, 673−684.

(5) Rawson, J. M.; Alberola, A.; Whalley, A. *J. Mater. Chem.* **2006**, *16*, 2560−2575.

(6) Jankowiak, A.; Pociecha, D.; Szczytko, J.; Monobe, H.; Kaszyński, P. *J. Am. Chem. Soc.* **2012**, *134*, 2465−2468.

(7) Wong, J. W. L.; Mailman, A.; Lekin, K.; Winter, S. M.; Yong, W.; Zhao, J.; Garimella, S. V.; Tse, J. S.; Secco, R. A.; Desgreniers, S.; Ohishi, Y.; Borondics, F.; Oakley, R. T. *J. Am. Chem. Soc.* **2014**, *136*, 1070−1081.

(8) Awaga, K.; Nomura, K.; Kishida, H.; Fujita, W.; Yoshikawa, H.; Matsushita, M. M.; Hu, L.; Shuku, Y.; Suizu, R. *Bull. Chem. Soc. Jpn.* **2014**, *87*, 234−249.

(9) Preuss, K. E. *Dalton Trans.* **2007**, 2357−2369.

(10) Sorai, M.; Nakazawa, Y.; Nakano, M.; Miyazaki, Y. *Chem. Rev.* **2013**, *113*, PR41−PR122.

(11) Steinberger, S.; Mishra, A.; Reinold, E.; Levichkov, J.; Uhrich, C.; Pfeiffer, M.; Baüerle, P. *Chem. Commun.* **2011**, *47*, 1982−1984.

(12) Kono, T.; Kumaki, D.; Nishida, J.; Tokito, S.; Yamashita, Y. *Chem. Commun.* **2010**, *46*, 3265−3267.

(13) Karikomi, M.; Kitamura, C.; Tanaka, S.; Yamashita, Y. *J. Am. Chem. Soc.* **1995**, *117*, 6791−6792.

(14) Mailman, A.; Winter, S. M.; Yu, X.; Robertson, C. M.; Yong, W.; Tse, J. S.; Secco, R. A.; Liu, Z.; Dube, P. A.; Howard, J. A. K.; Oakley, R. T. *J. Am. Chem. Soc.* **2012**, *134*, 9886−9889.

(15) Leitch, A. A.; Lekin, K.; Winter, S. M.; Downie, L. E.; Tsuruda, H.; Tse, J. S.; Mito, M.; Desgreniers, S.; Dube, P. A.; Zhang, S.; Liu, Q.; Jin, C.; Ohishi, Y.; Oakley, R. T. *J. Am. Chem. Soc.* **2011**, *133*, 6051−6060.

(16) Winter, S. M.; Mailman, A.; Oakley, R. T.; Thirunavukkuarasu, K.; Hill, S.; Graf, D. E.; Tozer, S. W.; Tse, J. S.; Mito, M.; Yamaguchi, H. *Phys. Rev. B* **2014**, *89*, 214403−1−214403−11.

(17) Winter, S. M.; Datta, S.; Hill, S.; Oakley, R. T. *J. Am. Chem. So.* **2011**, *133*, 8126−8129.

(18) Alberola, A.; Less, R. J.; Pask, C. M.; Rawson, J. M.; Palacio, F.; Oliete, P.; Paulsen, C.; Yamaguchi, A.; Farley, R. D.; Murphy, D. M. *Angew. Chem., Int. Ed.* **2003**, *42*, 4782−4785.

(19) Lekin, K.; Hoa, P.; Winter, S. M.; Wong, J. W. L.; Leitch, A. A.; Laniel, D.; Yong, W.; Secco, R. A.; Tse, J. S.; Desgreniers, S.; Dube, P. A.; Shatruk, M.; Oakley, R. T. *J. Am. Chem. Soc.* **2014**, *136*, 8050−8062.

(20) Hoa, P.; Lekin, K.; Winter, S. M.; Oakley, R. T.; Shatruk, M. *J. Am. Chem. Soc.* **2013**, *135*, 15674−15677.

(21) Preuss, K. E. *Coord. Chem. Rev.* **2014**, DOI: 10.1016/j.ccr.2014.09.016.

(22) Markovskii, L. N.; Kornuta, P. P.; Kachkovskaya, L. S.; Polumbrik, O. M. *Sulfur Lett.* **1983**, *1*, 143−145.




DOI: 10.1021/acs.cgd.5b00296
*Cryst. Growth Des.* XXXX, XXX, XXX−XXX

(23) Hayes, P. J.; Oakley, R. T.; Cordes, A. W.; Pennington, W. T. *J. Am. Chem. Soc.* **1985**, *107*, 1346−1351.
(24) Cordes, A. W.; Hayes, P. J.; Josephy, P. D.; Koenig, H.; Oakley, R. T.; Pennington, W. T. *J. Chem. Soc., Chem. Commun.* **1984**, 1021−1022.
(25) Boeré, R. T.; Oakley, R. T.; Reed, R. W.; Westwood, N. P. C. *J. Am. Chem. Soc.* **1989**, *111*, 1180−1185.
(26) Boeré, R. T.; Roemmele, T. L.; Yu, X. *Inorg. Chem.* **2011**, *50*, 5123−5136.
(27) Ang, C. Y.; Boeré, R. T.; Goh, L. Y.; Koh, L. L.; Kuan, S. L.; Tan, G. K.; Yu, X. *Chem. Commun.* **2006**, 4735−4737.
(28) Ang, C. Y.; Kuan, S. L.; Tan, G. K.; Goh, L. Y.; Roemmele, T. L.; Yu, X.; Boeré, R. T. *Can. J. Chem.* **2015**, *93*, 181−195.
(29) Bacon, C. E.; Eisler, D. J.; Melen, R. L.; Rawson, J. M. *Chem. Commun.* **2008**, 4924−4926.
(30) Leitch, A. A.; Korobkov, I.; Assoud, A.; Brusso, J. L. *Chem. Commun.* **2014**, *50*, 4934−4936.
(31) Oakley, R. T.; Reed, R. W.; Cordes, A. W.; Craig, S. L.; Graham, J. B. *J. Am. Chem. Soc.* **1987**, *109*, 7745−7749.
(32) Peak, D. A. *J. Chem. Soc.* **1952**, 215−226.
(33) Cordes, A. W.; Bryan, C. D.; Davis, W. M.; Delaat, R. H.; Glarum, S. H.; Goddard, J. D.; Haddon, R. C.; Hicks, R. G.; Kennepohl, D. K.; Oakley, R. T.; Scott, S. R.; Westwood, N. P. C. *J. Am. Chem. Soc.* **1993**, *115*, 7232−7239.
(34) Brown, H. C.; Schuman, P. D. *J. Org. Chem.* **1963**, *2*, 1122−1127.
(35) Bisson, J.; Dehaudt, J.; Charbonnel, M.-C.; Guillaneux, D.; Miguirditchian, M.; Marie, C.; Boubals, N.; Dutech, G.; Pipelier, M.; Blot, V.; Dubreuil, D. *Chem.—Eur. J.* **2014**, *20*, 7819−7829.
(36) Boeré, R. T.; Roemmele, T. L. *Phosphorus, Sulfur Silicon Relat. Elem.* **2004**, *179*, 875−882.
(37) Meyer, B. *Chem. Rev.* **1976**, *76*, 367−388.
(38) Zefirov, Y. V.; Zorkii, P. M. *J. Struct. Chem.* **1976**, *17*, 644−645.
(39) Ernest, I.; Holick, W.; Rihs, G.; Schomburg, D.; Shoham, G.; Wenkert, D.; Woodward, R. B. *J. Am. Chem. Soc.* **1981**, *103*, 1540−1544.
(40) Sharma, B. D.; Donohue, J. *Acta Crystallogr.* **1963**, *16*, 891−897.
(41) Zefirov, Y. V.; Zorkii, P. M. *Zh. Strukt. Khim.* **1976**, *17*, 745−756.
(42) Chakraborti, A. K.; Kaur, G.; Roy, S. *Indian J. Chem. Sec. B* **2001**, *40*, 1000−1006.
(43) Zhang, N.; Ayral-Kaloustian, S.; Nguyen, T.; Hernandez, R.; Lucas, J.; Discafani, C.; Beyer, C. *Bioorg. Med. Chem.* **2009**, *17*, 111−118.
(44) *WinEPR Simfonia*, version 1.25; Bruker Instruments, Inc.: Billerica, MA, 1996.
(45) *APEX Software Suite*, v.2012; Bruker AXS: Madison, WI, 2005.
(46) Blessing, R. H. *Acta Crystallogr., Sect. A* **1995**, *51*, 33−38.
(47) Sheldrick, G. M. *Cell_Now*; Bruker-AXS: Madison, WI, 2004.
(48) Sheldrick, G. M. *Acta Crystallogr., Sect. A* **2008**, *64*, 112−122.



DOI: 10.1021/acs.cgd.5b00296
*Cryst. Growth Des.* XXXX, XXX, XXX−XXX